In vivo absorption spectroscopy of tumor sensitizers with femtosecond white light

af Klinteberg, C; Pifferi, A; Andersson-Engels, Stefan; Cubeddu, R; Svanberg, Sune

Published in:
Applied Optics

2005

In vivo absorption spectroscopy of tumor sensitizers with femtosecond white light

Claes af Klinteberg, Antonio Pifferi, Stefan Andersson-Engels, Rinaldo Cubeddu, and Sune Svanberg

A system based on a femtosecond white-light continuum and a streak camera was used for recordings of the *in vivo* absorption spectra of the tumor-seeking agent disulphonated aluminum phthalocyanine. Measurements for different drug doses were performed on tumor tissue (muscle-implanted adenocarcinoma) and normal muscle tissue in rats. It was found that the shape of the spectrum is tissue dependent. The peak of the absorption spectrum is blueshifted in tumor tissue as compared with the muscle. Thus the contrast in the drug-related absorption can be altered by up to a factor of 2 from the primary drug molecular-concentration contrast between normal muscle and tumor by the proper selection of the illumination wavelength.

OCIS codes: 170.6510, 170.5180.

1. Introduction

During the past decades photodynamic therapy (PDT) has attracted much attention as a developing tumor treatment modality. It is based on the administration of a photosensitizing dye, which is selectively accumulated in tumor tissue, followed by exposure of the tissue with light within the wavelength range absorbed by the dye. For most photosensitizers an absorption maximum in the red part of the spectrum is used for the treatment. To achieve optimal treatment efficacy, it is important to choose a wavelength corresponding to the absorption peak. Consequently, it is important to gain knowledge on the absorption spectrum of the dye. With broadband light sources, such as filtered lamps, it is easy to cover the absorption peak. However, much of the treatment light will not be efficiently absorbed by the photosensitizer but rather by tissue chromophores, leading to a temperature increase. With a laser tuned to the right wavelength, the energy will efficiently be used for PDT and the temperature increase can be kept at a minimum.

To find the optimal wavelength, it is important to determine the absorption spectrum *in vivo* since the absorption peak is often shifted due to the functional state, metabolism, or blood perfusion. Several researchers have demonstrated that, for a hematoporphyrin derivative (HpD) and PHOTOFRIN, the absorption spectrum,[1] the action spectrum,[2,3] and the fluorescence excitation spectrum[4] all have a maximum at 625 nm *in vivo*, as compared with 630 nm for the action spectrum *in vitro*.[5] To optimize the PDT efficacy, one would like to know the action spectrum of the photosensitizer *in situ*. A complication is that the action spectrum can be evaluated only as an average of many treatments. To optimize each individual treatment, one would like to obtain a good approximation of the action spectrum for the photosensitizer in the tissue to be treated. An important finding is thus the similarity between the action spectrum and the fluorescence excitation and absorption spectra, since the latter two can be obtained from single samples. For cellular studies, fluorescence excitation spectroscopy has advantages over direct absorption spectroscopy, particularly because of the higher sensitivity and the reduction of light-scattering problems. For *in vivo* measurements, the multiple-scattering properties of the tissue normally cause a strong interaction between the absorption and the scattering properties. In this paper we demonstrate a novel technique that is used to determine

C. Klinteberg, S. Andersson-Engels, and S. Svanberg (sune.svanberg@fysik.lth.se) are with the Department of Physics, Lund Institute of Technology, P.O. Box 118, Lund S-221 00, Sweden. A. Pifferi and R. Cubeddu are with the Department of Physics, Centro Elettronica Quantistica e Strumentazione Elettronica—Consiglio Nazionale delle Ricerche and INFM, Politecnico di Milano, Piazza Leonardo da Vinci, Milan I-20133, Italy.

Received 7 July 2004; revised manuscript received 5 December 2004; accepted 6 December 2004.

0003-6935/05/112213-08$15.00/0

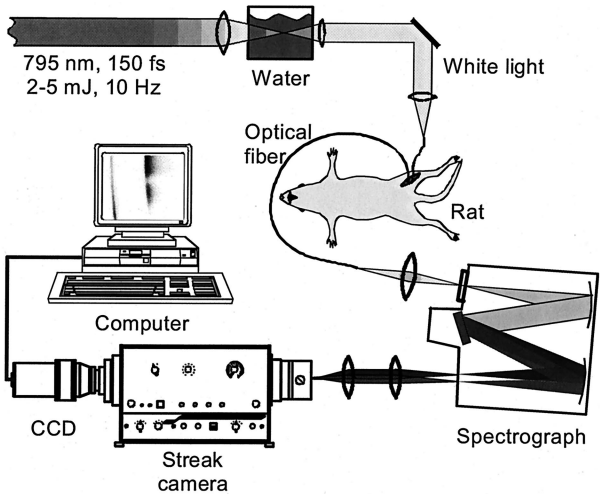

Fig. 1. Schematic of the experimental setup.

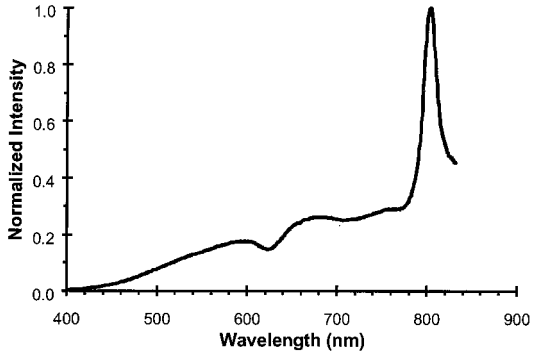

Fig. 2. Intensity spectrum of the white light.

the *in vivo* absorption spectrum from the transmission signal following short pulsed white-light illumination using time-resolved techniques.[6] By using time- and wavelength-resolved detection, we can obtain the temporal dispersion of the diffusely scattered light as a function of wavelength over a large wavelength region in a single measurement, and the absorption spectrum can be evaluated in spite of the scattering complications. In this way the true selectivity of drug uptake in tumor tissue can be assessed.

In this paper we use the technique outlined above to determine the *in vivo* absorption spectrum between 600 and 800 nm of a phtalocyanine in tumor and muscle tissue of rats. Differences in the absorption spectrum between the different tissue types were investigated.

2. Experimental Setup

We studied time-resolved diffuse reflectance using femtosecond white-light pulses. The experimental setup is schematically shown in Fig. 1. As a light source, a tabletop terawatt laser in Lund was used. The laser system is described in detail elsewhere.[7] In short, it was based on an argon-ion laser-pumped, passively mode-locked Ti:sapphire laser, operating at a repetition rate of 76 MHz, with a pulse length of approximately 150 fs and a Fourier-limited spectral profile centered on 792 nm. The laser pulses were stretched in time with a pair of gratings and amplified in two steps with Nd:YAG laser-pumped Ti:sapphire crystals. Finally, the pulses were recompressed to a pulse length of ~150 fs. Thus it was possible to obtain pulses with a peak power of ~1 TW, at a repetition rate of 10 Hz. In the present study, we used a maximum pulse energy of ~5 mJ.

We focused the high-power laser pulses into a 5-cm-long cuvette of water using a lens with a focal length of 15 cm. Nonlinear effects, such as self-phase modulation of the refractive index due to the high peak power, resulted in an instantaneous frequency shift proportional to the time derivative of the intensity. As a result, almost structureless light pulses covering the whole visible and near-infrared wavelength region were obtained (Fig. 2). The dip that can be seen at ~630 nm is due to the inverse Raman effect in water.[8] The white-light radiation was collimated with a 50-mm camera lens and then focused into a 600-μm-diameter optical fiber. The polished distal end of the fiber was held in gentle contact with the tissue under investigation. The diffusely backscattered light was collected with another fiber of the same kind. Both fibers were mounted in a fiber holder, making it possible to keep the fibers parallel to each other and to keep the interfiber distance fixed between measurements. We then spectrally dispersed the collected light in a 27-cm spectrograph (SPEX Model 270M) using a grating with 150 grooves/mm. Two camera lenses, with a focal length of 135 and 50 mm, respectively, were used to image the output plane of the spectrograph onto the entrance slit of a streak camera (Hamamatsu C1587). A small fraction of the white light was split off by means of a glass plate, bypassed the tissue under investigation, and guided directly to the spectrograph with a 200-μm-diameter optical fiber. When we adjusted the path length for this light, it arrived to the streak camera approximately 0.5 ns before the diffusely scattered light. This light pulse was used as a time reference. The streak camera allowed time-resolved detection of the wavelength-dispersed light. A charge-coupled device (CCD) camera, thermoelectrically cooled to −30 °C, was used to capture images with intensity as a function of time (x axis) and wavelength (y axis). In principle, it was possible to acquire time-dispersion curves for all wavelengths in the visible and near-infrared region with a single laser pulse. Because of the limited electron current through the streak camera tube, the diffusely reflected light from 600 laser pulses was accumulated to obtain a good signal-to-noise ratio. The images from the CCD camera were transferred to a computer and stored for further evaluation.

The spectral resolution of the system, including the optical fibers and all other optical elements, was approximately 3 nm, and the temporal resolution was 30 ps when the streak camera was used in the accumulation mode.

3. Drug and Animals

Aluminum phthalocyanine with an average degree of sulphonation of 2.1 (hereafter called disulphonated aluminum phthalocyanine AlS_2Pc) was kindly provided by A. McLennan (Paisley College of Technology, Paisley, UK) and was diluted in saline to a concentration of 2.5 mg/ml. The degree of sulphonation was ascertained by means of chromatography. The compound consists of a mixture of isomers with sulphonic groups in both adjacent and opposite positions. The experiments were carried out with the approval of the local ethics committee.

Female white inbred Wistar-Furth rats were used for the experiment. A malignant tumor was induced on both hind legs by local inoculation of syngeneic tumor cells prepared from a colon adenocarcinoma, originally chemically induced by injection of dimethylhydrazine.[9] Seven to nine days prior to the investigation, 3×10^5 viable tumor cells were inoculated subcutaneously in both hind legs.

4. Data Evaluation

For each streak camera image, we obtained time-dispersion curves for every 10 nm by adding a certain number of rows. To compensate for the small nonlinearity of the time scale in the streak camera images, we properly linearized the time-dispersion curves prior to analysis using an interpolation procedure. We convolved a theoretical reflectance curve, as described in the diffusion model for a semi-infinite homogenous medium[10] using the extrapolated boundary conditions,[11] with the system impulse response; the curve was fitted to the data with the absorption coefficient μ_a and the reduced scattering coefficient μ_s' as free parameters. The impulse response was measured while the two fiber ends were facing each other and were kept in contact. The fitting range started at 10% of the maximum intensity on the leading edge and ended at 1% on the trailing edge. We obtained the best fitting parameters (μ_a and μ_s') by means of an iterative procedure to minimize the reduced χ^2 using the Levenberg–Marquardt algorithm.[12] To improve the robustness of the fit and to reduce fluctuations in the absorption spectrum, we repeated the fit varying both μ_a and a free time shift t_0, while keeping μ_s' fixed and equal to the average scattering spectrum obtained with the first fit. We have shown in a study on phantoms[13] that the μ_a–t_0 fitting method is rather insensitive to the estimate of μ_s', although it significantly improves the precision and accuracy of the absorption measurement, especially for short interfiber distances and high absorption values (as in this case). All the spectra presented in the following on the AlS_2Pc absorption were obtained with this analysis technique. The results, although more noisy, were fully confirmed with the standard fitting method with μ_a and μ_s' as free parameters (data not shown).

Use of white-light excitation and the evaluation method discussed above has as a prerequisite that the recorded scattered radiation is not contaminated with wavelength-shifted fluorescence light. Such effects due to chlorophyll fluorescence have been observed in white-light experiments of photon propagation in leaves.[14] However, strong absorption leading to fluorescence occurs only for wavelengths below 420 nm for AlS_2Pc, where the white-light intensity, according to Fig. 2, from our source is negligible. Thus no evidence for fluorescence contamination was observed.

5. Measurements

Measurements for muscle tissue were performed twice on nine hind legs of six rats, resulting in 18 images. Both tumors on seven animals were measured twice (28 images) before injection of the sensitizer. The average spectra of all the control measurements were calculated for the two different tissue types (tumor and muscle) and were used to represent the endogenous tissue absorption.

The rats were injected intraperitonially with AlS_2Pc at a dose of either 2.5 or 5 mg/kg body weight (b.w.), and the measurements were performed 2 to 6 h later. For the lower dose (2.5 mg/kg b.w.), ten measurements were performed on five muscles of three rats and eight measurements were performed on four tumors of two rats. At the higher dose (5 mg/kg b.w.), the numbers for muscle tissue were the same, whereas two more tumors in one rat were measured, resulting in a total of 12 measurements.

To determine the *in vivo* absorption spectrum of the sensitizer, the following procedure was employed. For each absorption spectrum obtained from the sensitized tissue, the contribution from the endogenous absorption was subtracted. The shape of the average absorption spectrum of the same tissue type prior to the injection of the sensitizer was used. Before the subtraction, the intensity of the average endogenous spectrum was scaled to the spectrum evaluated with the absorption above 840 nm set equal, i.e., assuming that there is no absorption of the sensitizer in this wavelength region. Then the resulting spectra were normalized to unity at the peak of the absorption curve. Next, all spectra belonging to the same group were averaged, and the standard errors were calculated. In this way the average shape of the spectrum was obtained. Finally, the average spectra and the errors were rescaled with the height of the absorption peak set equal to the average of the maximum value of the background-free curves before normalization. This final operation allowed us to display the average value of the peak absorption.

6. Results

A typical streak camera image of the diffusely backscattered white light in the muscle of the hind leg, with a distance between the source and the detector fibers of 8 mm, is shown in Fig. 3. The intensity is shown on a gray scale as a function of time and wavelength. As a result of the absorption peak of AlS_2Pc, a decrease in the intensity and also a narrowing of the time dispersion can be seen for wavelengths around 680 nm. Time-dispersion curves for light of

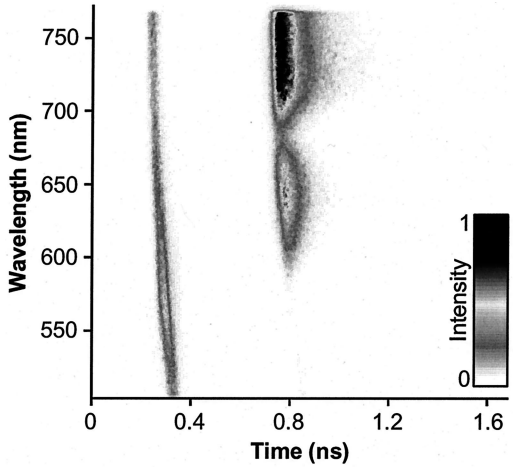

Fig. 3. Typical streak camera image recorded in the muscle of the hind leg 4 h postintraperitonial injection of AlS_2Pc (5 mg/kg b.w.).

different wavelengths can be obtained as cross sections through the streak camera image.

An example of the result of the fitting procedure is shown in Fig. 4. The impulse response of the system (filled diamonds) is convoluted with the solution to the diffusion equation in a semi-infinite medium, which results in a theoretical reflection curve (solid curve). This model is fitted to the data (open circles) to obtain the absorption coefficient. When we repeat this procedure every 10 nm in the wavelength scale of one image, an absorption spectrum can be assessed. After averaging all the spectra from the photosensitizer-free tissue, the background absorption of the two tissue types was obtained (Fig. 5). Both spectra show a decreasing absorption with increasing wavelength that is typical of the absorption contribution of deoxyhemoglobin in this wavelength range. The small peak at 760 nm is again due to the deoxyhemoglobin whereas the small shoulder around 640 nm is not related to hemoglobin. As can be seen in Fig. 5, the absorption is higher in tumor tissue (filled symbols) than in muscle tissue (open symbols). The relative increase in absorption is more evident in the red region of the spectrum ($\lambda < 700$ nm) where it is ~30–50%, whereas it is less pronounced in the near

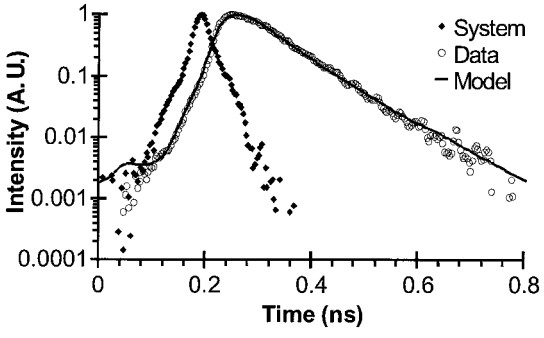

Fig. 4. Typical result of the evaluation procedure. The impulse response of the system (filled diamonds) is convoluted to the solution of the diffusion equation. This gives a theoretical model (solid curve), which is fitted to the data (open circles).

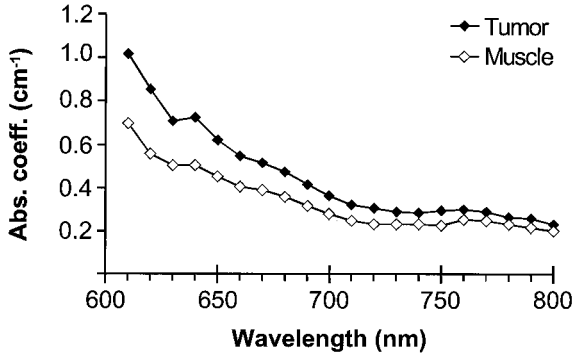

Fig. 5. Absorption spectra of rodent tumor (filled symbols) and muscle (open symbols) without any photosensitizer. The error bars are approximately ±0.03 around 670 nm and become larger toward the blue region as reflected in the data shown in Fig. 8.

infrared ($\lambda > 750$ nm) where it is only 15–20%. The corresponding scattering spectra are shown in Fig. 6. The reduced scattering decreases with increasing wavelength, from 15 cm^{-1} down to 11 cm^{-1}. The scattering spectra in the tumor and in the normal muscle are quite similar. A slightly higher value (~5–10%) was found in the muscle.

A typical absorption spectrum obtained in tumor tissue following phtalocyanine administration is shown in Fig. 7. In Fig. 7(a) the spectrum calculated from the experimental data (solid curve) and the corresponding endogenous absorption of tumor tissue without any photosensitizer (dashed curve) are shown. By subtracting the endogeneous absorption from the recorded spectrum, we obtain the *in vivo* absorption spectrum of AlS_2Pc [Fig. 7(b)].

The average spectra obtained in the two tissue types after intraperitonial injection of two different doses (2.5 and 5.0 mg/kg b.w.) of the sensitizer are shown in Fig. 8. In terms of line shape, the spectrum in the tumor is blueshifted as compared with the one measured in the muscle. At the lower drug dose, the absorption spectrum peaks around 690 nm for the muscle and between 680 and 690 nm for the tumor. This difference is even more marked at the higher drug dose, for which the absorption peaks at 680 nm

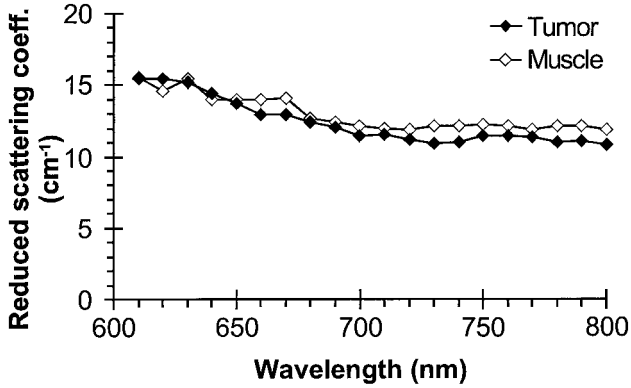

Fig. 6. Reduced scattering spectra of rodent tumor (filled symbols) and muscle (open symbols) without any photosensitizer.

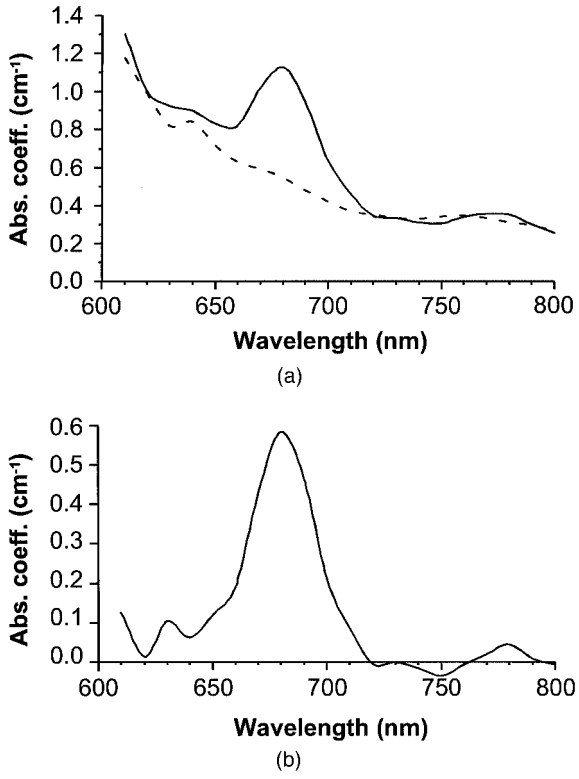

Fig. 7. (a) Absorption spectrum of a tumor 4 h postintraperitonial injection of AlS_2Pc (2.5 mg/kg b.w.). The background absorption from the tissue is shown as a dashed curve. (b) The resulting *in vivo* absorption spectrum after we subtracted the tissue absorption from the result shown in (a).

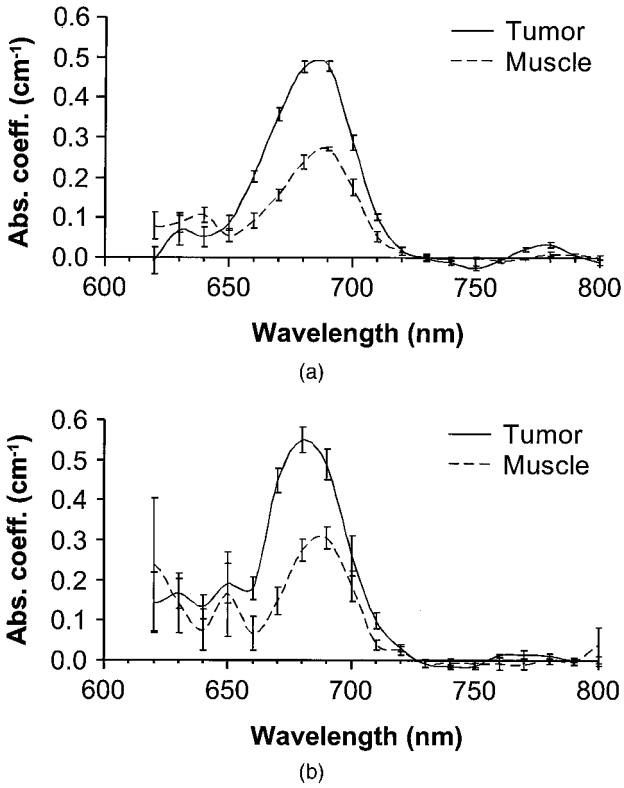

Fig. 8. Resulting *in vivo* absorption spectra from rodent tissue after intraperitonial injection of AlS_2Pc at a dose of (a) 2.5 mg/kg b.w., and (b) 5.0 mg/kg b.w. The absorption of the sensitizer in tumor tissue (solid curves) is approximately twice that obtained in the muscle tissue (dashed curve). Moreover, the absorption spectra obtained in the muscle are redshifted. No difference in absorption coefficient could be found between the two doses, however.

in the tumor. In terms of absolute values, the drug absorption in the tumor is approximately twice that obtained in the normal tissue for both drug doses, and the peak values seem to be rather independent of the drug dose.

7. Discussion

There are several possibilities for measurement of the absorption spectrum of a photosensitizer. For measurements in solutions, a spectrophotometer can be used. This instrument can also be used to determine the absorption spectrum of the photosensitizer in, e.g., blood serum. One limitation with such measurements in biological tissues and fluids is the scattering, making the optical path length through a measurement cuvette undetermined. It is not possible to use the spectrophotometer for *in vivo* measurements of solid tissue. For this purpose, Patterson *et al.* proposed the possibility of using diffusely reflected light.[15] By illuminating the tissue with continuous-wave white light from an optical fiber, and collecting the light at various distances using several other fibers, we can calculate the optical properties of the tissue (absorption and scattering coefficients),[16–19] e.g., with the steady-state diffusion equation model. Potential limitations of this method are, for example, the sensitivity to boundary conditions at the tissue surface, finite tissue volumes, and the number of measurement points needed that might lead to significant errors due to tissue heterogeneity. On the other hand, the instrumentation is relatively straightforward and inexpensive, and the measurements can be performed in real time. An alternative method is to perform time-resolved measurements of the local diffuse reflectance. Since only two fibers are needed, the measurement is less sensitive to tissue inhomogeneities because there is no need to correlate measurements at different interfiber distances. Also, the tissue volume probed can be fairly small. Depending on the optical properties of the tissue and the time resolution of the system, the two fibers can be relatively close together, ≤ 1 cm. The drawback with this approach is that usually a tunable laser is needed, and the measurements at different wavelengths must be performed sequentially.[20] This can significantly increase the measurement time. Also, independent laser sources may be needed to cover wide spectral ranges. Moreover, the instrumentation is more complex and expensive than for steady-state measurements.

Knowledge of the *in vivo* absorption spectrum of photosensitizers used for PDT is important so that the right wavelength of the treatment light is chosen.

It has been shown by several authors that HpD and PHOTOFRIN exhibit a blueshift of the absorption with 5 nm (from 630 to 625 nm) *in vivo* as compared with an aqueous solution.[4] Even though the shift is rather small, it should be noted that clinical protocols usually prescribe a treatment wavelength of 630 ± 3 nm. Thus 633 nm would in principle be acceptable, but because of the relatively narrow peak of the *in vivo* action spectrum of HpD[2], the treatment effect would be considerably reduced. For AlS_2Pc, on the other hand, the absorption peak is redshifted approximately 10–15 nm (see Fig. 8).[21] This is in agreement with several previously published investigations on sulphonated metallo-phthalocyanines. Griffiths *et al.* reported an increased PDT effect when the wavelength of the activating light was increased from 680 to 692 nm using zinc phthalocyanine tetrasulphonic acid.[22] Similar results have also been reported by Cubeddu *et al.*[21] for AlS_2Pc, where the *in vivo* absorption spectrum peaked at 685 nm compared with 672 nm for absorption in aqueous solution[23] and cell cultures.[24] Furthermore, Weersink *et al.*[19] found a redshift to ~680 nm of the absorption peak of tetrasulphonated aluminum phthalocyanine (AlS_4Pc) in rabbit skin, which is in agreement with the findings for AlS_2Pc. Stratonnikov *et al.*,[18] however, found a redshift of the absorption peak of Photosence (NIOPIC, Russia) in human lip *in vivo* of only 4 nm, as compared with the aqueous solution. Photosence is a mixture consisting of ~30% tetrasulphonated, 50% trisulphonated, and 20% disulphonated aluminum phthalocyanine.[25]

Another finding in this study is that the absorption peak is slightly blueshifted for the tumor as compared with the muscle tissue (Fig. 8). Cubeddu *et al.*[26] have shown that, for cells of an ascitic tumor (L1210 lymphoid leukemia) incubated with AlS_2Pc *ex vivo*, the redshift of the absorption peak decreases with increasing concentration. One explanation for this could be a saturation effect at higher doses, meaning that some sensitizer molecules are not strictly bound to the cells. Hence they experience an environment similar to the aqueous one, and the absorption peak will be at 670–675 nm. In this study we note that the absorption peak appeared at longer wavelengths for muscle tissue than for tumor tissue. Furthermore, the peak absorption coefficient was approximately half of that found in tumor tissue, indicating a lower concentration of the sensitizer. This might suggest that the amount of free sensitizer molecules is lower in muscle tissue, resulting in a larger redshift, which is in agreement with the findings *ex vivo*.[26] Moreover, we have observed that, increasing the drug dose from 2.5 to 5.0 mg/kg b.w., the key effect is a blueshift of the absorption spectrum with minor changes in peak value [see Fig. 8(b)]. This behavior seems to confirm a saturation effect at high drug concentrations due to a filling up of the available binding sites for AlS_2Pc within the tissue. These concentration-dependent variations in the absorption spectrum might be exploited to increase selectivity for PDT treatment.

Table 1. *In vivo* Absorption Coefficient of AlS_2Pc in Tumor and Normal Rat Muscle Obtained at Two Wavelengths (670 and 690 nm) Following Intraperitonial Injection of Two Different Doses (2.5 and 5.0 mg/kg b.w.)[a]

	Dose: 2.5 mg/kg		Dose: 5.0 mg/kg	
Protocol	670 nm	690 nm	670 nm	690 nm
Drug μ_a in muscle (cm^{-1})	0.16	0.27	0.15	0.30
Drug μ_a in tumor (cm^{-1})	0.36	0.48	0.45	0.49
Contrast	2.3	1.8	3.1	1.6

[a]The absorption contrast between tumor and muscle is also presented.

Spectral filtering due to tissue chromophores can influence the shape of fluorescence spectra as described by Swartling *et al.*[27] However, since the present measurements concern absorption, and since the differential absorption due to the sensitizer is observed as a difference between the same type of tissue, with and without a sensitizer, no spectral modifications in the sensitizer absorption due to other chromophores are expected.

In Table 1 we report the contrast in AlS_2Pc absorption in the tumor as compared with the normal tissue calculated at 670 and 690 nm from the data in Fig. 8. The contrast is dependent on both drug dose and irradiation wavelength and varies from 1.6 at 690 nm with a drug dose of 5 mg/kg b.w. up to a maximum of 3.1 at 670 nm with the same drug dose. Clearly, the choice of the treatment protocol should also take into account aspect other than contrast, such as the absorption coefficient at the irradiating wavelength that must be combined with the irradiating modalities, the maximum acceptable drug dose, and so on. On the other hand, the free sensitizer molecules might not cause any photodynamic damage if they are not close to any vital part of the cells. Thus the treatment effect must be evaluated separately. Yet we have shown that the shape of the absorption spectrum of the photosensitizer is an aspect to be investigated, since it can be significantly altered under different operating conditions.

In this respect, one major advantage with the technique described in this paper is the possibility to obtain the data for all wavelengths simultaneously, with an overall acquisition time of 1–2 min for the whole spectrum. This is important, especially for *in vivo* measurements, since any changes in the status of the tissue, the pharmacokinetics of the accumulation of the photosensitizer, and position of the measurement probe will affect the total measurement. Moreover, the wide spectrum obtained with a femtosecond supercontinuum allows one to derive the optical properties of the tissue under study far beyond the region where the drug absorbs. Thus it is possible to use the tails of the absorption spectrum to extrapolate the contribution of the drug-free tissue that can be subtracted to obtain the background-free photosensitizer absorption. Since there are relevant intersubject variations and time-related changes of the

tissue absorption, primarily due to changes in blood content and oxygenation, the possibility to evaluate the background contribution at the time of measurement is of great advantage. Clearly, the system described is not suitable for clinical use. However, with recent developments regarding more efficient white-light generation, further discussed in Section 8, compact and realistic measurements systems could be built. Alternatively, once the wavelengths of interests, and the parameters to be tracked, have been properly identified with a white-light system, a compact time-resolved reflectance instrumentation can be devised by use of a few laser diodes at selected wavelengths and a PC board for time-correlated single-photon counting. This solution was successfully used, for example, to monitor blood oxygenation with a compact system.[28–31]

8. Conclusions

We have used a system based on a femtosecond white-light continuum and a streak camera for the *in vivo* measurement of absorption spectra in the wavelength range from 600 to 800 nm of AlS_2Pc in rats comparing different tissue types (muscle and muscle-implanted adenocarcinoma) and drug doses. In this way the selective uptake of the drug can be measured in an unambigous way, in contrast to the case when, e.g., fluorescence is monitored. The shape of the spectrum depends on the drug uptake in the tissue with a blueshift of the peak from 690 down to 680 nm passing from the muscle to the tumor at the drug dose of 5.0 mg/kg b.w. Consequently, the contrast in the drug-related absorption can be altered by up to a factor of 2 from the primary drug molecular-concentration contrast between normal muscle and tumor by properly selecting the illumination wavelength. Similar techniques have recently been used to study constituents in pharmaceutical tablets.[32]

Future white-light absorption measurements of the kind reported in this paper can be made compact taking advantage of the recent development of photonic bandgap fibers, enabling efficient white-light generation also with low-energy and high-repetition-rate femtosecond laser sources.[33,34]

The authors thank Gianfranco Canti and Ingrid Wang for help with the animals. This research was financially supported by the European Community Access to Large Scale Facilities Program (contract ERBFMGECT950020) and the Knut and Alice Wallenberg Foundation.

References

1. R. Cubeddu, G. Canti, M. Musolino, A. Pifferi, P. Taroni, and G. Valentini, "Absorption-spectrum of hematoporphyrin derivative in-vivo in a murine tumor-model," Photochem. Photobiol. **60,** 582–585 (1994).
2. W. M. Star, J. Versteeg, W. van Putten, and H. Marijnissen, "Wavelength dependence of hematoporphyrin derivative photodynamic treatment effects on rat ears," Photochem. Photobiol. **52,** 547–554 (1990).
3. T. J. Farrell, M. C. Olivo, M. S. Patterson, H. Wrona, and B. C. Wilson, "Investigation of the dependence of tissue necrosis on irradiation wavelength and time post injection using a photodynamic threshold dose model," in *Photodynamic Therapy and Biomedical Lasers*, P. Spinelli, M. Dal Fante, and R. Marchesini, eds. (Elsevier, Amsterdam, 1992), pp. 830–834.
4. G. H. M. Gijsbers, D. Breederveld, M. J. C. van Gemert, T. A. Boon, J. Langelaar, and R. P. H. Rettschnick, "*In vivo* fluorescence excitation and emission spectra of hematoporphyrin-derivative," Lasers Life Sci. **1,** 29–48 (1986).
5. C. J. Gomer, D. R. Doiron, N. Rucker, N. J. Razum, and S. W. Fountain, "Action spectrum (620–640 nm) for hematoporphyrin derivative induced cell killing," Photochem. Photobiol. **39,** 365–368 (1984).
6. S. Andersson-Engels, R. Berg, A. Persson, and S. Svanberg, "Multispectral tissue characterization with time-resolved detection of diffusely scattered white light," Opt. Lett. **18,** 1697–1699 (1993).
7. S. Svanberg, J. Larsson, A. Persson, and C. G. Wahlström, "Lund high-power laser facility—systems and first results," Phys. Scr. **49,** 187–197 (1994).
8. W. J. Jones and B. P. Stoicheff, "Inverse Raman spectra: induced absorption at optical frequencies," Phys. Rev. Lett. **13,** 657–659 (1964).
9. G. Hedlund and H. O. Sjögren, "Induction of transplantation immunity to rat colon carcinoma isografts by implantation of intact fetal colon tissue," Int. J. Cancer **26,** 71–73 (1980).
10. M. S. Patterson, B. Chance, and B. C. Wilson, "Time resolved reflectance and transmittance for the noninvasive measurement of optical properties," Appl. Opt. **28,** 2331–2336 (1989).
11. R. C. Haskell, L. O. Svaasand, T.-T. Tsay, T.-C. Feng, M. S. McAdams, and B. J. Tromberg, "Boundary conditions for the diffusion equation in radiative transfer," J. Opt. Soc. Am. A **11,** 2727–2741 (1994).
12. W. H. Press, S. A. Teukolsky, W. T. Vetterling, and B. P. Flannery, *Numerical Recipes in C: The Art Of Scientific Computing* (Cambridge U. Press, New York, 1992).
13. R. Cubeddu, A. Pifferi, P. Taroni, A. Torricelli, and G. Valentini, "Experimental test of theoretical models for time-resolved reflectance," Med. Phys. **23,** 1625–1633 (1996).
14. J. Johansson, R. Berg, A. Pifferi, S. Svanberg, and L. O. Björn, "Time-resolved studies of light propagation in Crassula and Phaseolus leaves," Photochem. Photobiol. **69,** 242–247 (1999).
15. M. S. Patterson, B. C. Wilson, J. W. Feather, D. M. Burns, and W. Pushka, "The measurement of dihematoporphyrin ether concentration in tissue by reflectance spectrophotometry," Photochem. Photobiol. **46,** 337–343 (1987).
16. T. J. Farrell, M. S. Patterson, and B. Wilson, "A diffusion theory model of spatially resolved, steady-state diffuse reflectance for noninvasive determination of tissue optical properties *in vivo*," Med. Phys. **19,** 879–888 (1992).
17. M. G. Nichols, E. L. Hull, and T. H. Foster, "Design and testing of a white-light, steady-state diffuse reflectance spectrometer for determination of optical properties of highly scattering systems," Appl. Opt. **36,** 93–104 (1997).
18. A. A. Stratonnikov, N. E. Edinca, D. V. Klimov, K. G. Linkov, V. B. Loschenov, E. A. Luckjanets, G. A. Meerovich, and E. G. Vakulovskaya, "The control of photosensitizer in tissue during photodynamic therapy by means of absorption spectroscopy," in *Photochemotherapy: Photodynamic Therapy and Other Modalities II*, S. B. Brown, B. Ehrenberg, and J. Moan, eds., Proc. SPIE **2924,** 49–60 (1996).
19. R. A. Weersink, J. E. Hayward, K. R. Diamond, and M. S. Patterson, "Accuracy of noninvasive *in vivo* measurements of photosensitizer uptake based on a diffusion model of reflectance spectroscopy," Photochem. Photobiol. **66,** 326–335 (1997).
20. R. Cubeddu, A. Pifferi, P. Taroni, A. Torricelli, and G. Valentini, "Noninvasive absorption and scattering spectroscopy of bulk diffusive media: an application to the optical character-

ization of human breast," Appl. Phys. Lett. **74,** 874–876 (1999).
21. R. Cubeddu, G. Canti, M. Musolino, A. Pifferi, P. Taroni, and G. Valentini, "*In vivo* absorption spectrum of disulphonated aluminium phthalocyanine in a murine tumour model," J. Photochem. Photobiol. B **34,** 229–235 (1996).
22. J. Griffiths, J. Cruse-Sawyer, S. R. Wood, J. Schofield, S. B. Brown, and B. Dixon, "On the photodynamic therapy action spectrum of zinc phthalocyanine tetrasulphonic acid *in vivo*," J. Photochem. Photobiol. B **24,** 195–199 (1994).
23. M. Ambroz, A. J. MacRobert, J. Morgan, G. Rumbles, M. S. C. Foley, and D. Phillips, "Time-resolved fluorescence spectroscopy and intracellular imaging of disulphonated aluminium phthalocyanine," J. Photochem. Photobiol. B **22,** 105–117 (1994).
24. J. Moan, K. Berg, J. C. Bommer, and A. Western, "Action spectra of phthalocyanines with respect to photosensitization of cells," Photochem. Photobiol. **56,** 171–175 (1992).
25. A. A. Stratonnikov, General Physics Institute, Moscow (personal communication, 2001).
26. R. Cubeddu, G. Canti, A. Pifferi, P. Taroni, A. Torricelli, and G. Valentini, "Study on the absorption properties of sulfonated aluminum phthalocyanine *in vivo* and *ex vivo* in murine tumor models," J. Biomed. Opt. **2,** 131–139 (1997).
27. J. Swartling, J. Svensson, O. Bengtsson, K. Terike, and S. Andersson-Engels, "Fluorescence spectra provide information on the depth of fluorescent lesions in tissue," Appl. Opt. **44,** 1934–1941 (2005).
28. M. Miwa, Y. Ueda, and B. Chance, "Development of a time-resolved spectroscopy system for quantitative noninvasive tissue measurements," in *Optical Tomography, Photon Migration and Spectroscopy of Tissue and Model Media: Theory, Human Studies, and Instrumentation*, B. Chance and R. R. Alfano, eds., Proc. SPIE **2389,** 142–149 (1995).
29. M. Oda, Y. Yamashita, G. Nishimura, and M. Tamura, "A simple and novel algorithm for time-resolved multiwavelength oximetry," Phys. Med. Biol. **41,** 551–562 (1996).
30. H. Zhang, Y. Tsuchiya, T. Urakami, M. Miwa, and Y. Yamashita, "Time integrated spectroscopy of turbid media based on the microscopic Beer-Lambert law: consideration of the wavelength dependence of scattering properties," Opt. Commun. **153,** 314–322 (1998).
31. R. Cubeddu, A. Pifferi, P. Taroni, A. Torricelli, and G. Valentini, "Compact tissue oximeter based on dual-wavelength multichannel time-resolved reflectance," Appl. Opt. **38,** 3670–3680 (1999).
32. J. Johansson, S. Folestad, M. Josefson, A. Sparén, C. Abrahamsson, S. Andersson-Engels, and S. Svanberg, "Time-resolved NIR/VIS spectroscopy for analysis of solids: pharmaceutical tablets," Appl. Spectrosc. **56,** 725–731 (2002).
33. J. K. Ranka, R. S. Windeler, and J. Stentz, "Visible continuum generation in air-silica microstructure optical fibers with anomalous dispersion at 800 nm," Opt. Lett. **25,** 25–27 (2000).
34. T. A. Birks, W. J. Wadsworth, and P. St. J. Russell, "Supercontinuum generation in tapered fibers," Opt. Lett. **25,** 1415–1417 (2000).